02

Analysis of raman spectra during excitation at wavelengths 532 and 785 nm for rapid skin tumors diagnosis

© I.N. Saraeva[1], E.N. Rimskaya[1], A.V. Gorevoy[1], A.B. Timurzieva[1,2], S.N. Shelygina[1], E.V. Perevedentseva[1], S.I. Kudryashov[1]

[1] Lebedev Physical Institute, Russian Academy of Sciences, 119991 Moscow, Russia
[2] „Semashko National Research Institute of Public Health", 105064 Moscow, Russia

e-mail: saraevain@lebedev.ru

Received December 11, 2023
Revised January 09, 2024
Accepted January 16, 2024

Raman microspectroscopy is an important method for skin cancer diagnosis in the early stages. The differentiation of malignant skin tumors (basal cell carcinomas of the skin, squamous cell carcinomas), benign skin tumors (papillomas) and healthy skin was carried out by acquiring Raman spectra *in vitro* with laser excitation at wavelengths of 532 and 785 nm and analyzing them using the principal component method. A comparison of the spectral features of the components with known peaks of molecular vibrations was carried out. It has been shown that differential diagnosis at an excitation wavelength of 785 nm is more reliable than at 532 nm, providing a probability of correct classification above 90%. The proposed methods can be applied for *in vivo* analysis for non-invasive rapid diagnostics using appropriate equipment for spectra registration.

Keywords: skin tumors, confocal scanning Raman microspectroscopy, principal component analysis method.

DOI: 10.61011/EOS.2024.01.58284.9-24

Introduction

Early detection of skin malignancies is an extremely important social problem in accordance with the statistical data on morbidity and mortality in the Russian Federation and abroad [1]. At early pathology stages, clinical manifestations of a neoplasm are mild and differential diagnosis is required, but, if no instrumentation is used, may be only provided by high qualified medical personnel. A final diagnosis is determined with high accuracy only using histologic examination of surgically removed tissues that may negatively affect the treatment efficacy [2]. Whilst the existing non-invasive methods and tools that are widely used in oncodermatology (dermatoscopy [3], thermometry [4], high-frequency ultrasonic skin scanning [5], cross-polarized optical coherent tomography [6], spectroscopy and terahertz visualization [7]) do not provide sufficient efficacy of early diagnosis [2,8]. The development of non-invasive express diagnosis methods for skin malignancies is an important issue whose solution will considerable increase the probability of early cancer detection and favorable treatment outcome.

Any changes in the tissue cell structure may be detected with high accuracy using the Raman scattering (RS) microspectroscopy therefore this procedure is widely used to distinguish different types of tumors. Some studies have reported successful distinguishing of skin malignancies from normal skin; thus, the authors of [9] proposed to distinguish Raman scattering spectra of basal cell carcinoma (BCC), squamous cell carcinoma (SCC), actinic keratosis induced by benign neoplasms and normal tissues using principal component analysis/discriminant analysis (PCA/DA) and partial least squares/discriminant analysis (PLS/DA) method. The obtained data have shown that spectral features of lipids and proteins may be efficiently used for the differential diagnosis. The algorithms distinguished the spectra of skin malignancies rom benign and normal tissues with an accuracy of 82.8% and 91.9%, respectively.

This study compares the performance of the principal component method for RS spectra analysis when using 532 nm and 785 nm excitation wavelengths in order to distinguish BCC, SCC and papilloma from normal skin. 532 nm laser emission excites unwanted intense fluorescence as opposed to 785 nm that helps minimize the background fluorescence of tissue and, therefore, may be ideal for the measurement of a fresh tissue [8,10,11]. Laser light penetration depth and degree of scattering depend both on the wavelength and tissue properties, therefore employment of various laser excitation wavelengths has good prospects. The addressed algorithms are universal and may be used both for *in vitro* analysis of surgically removed parts of skin and for *in vivo* analysis with noninvasive diagnosis using the appropriate equipment for RS spectra recording.

Experimental

Surgically removed normal skin areas and tumors with non-damaged tissue were used as test samples (5 normal

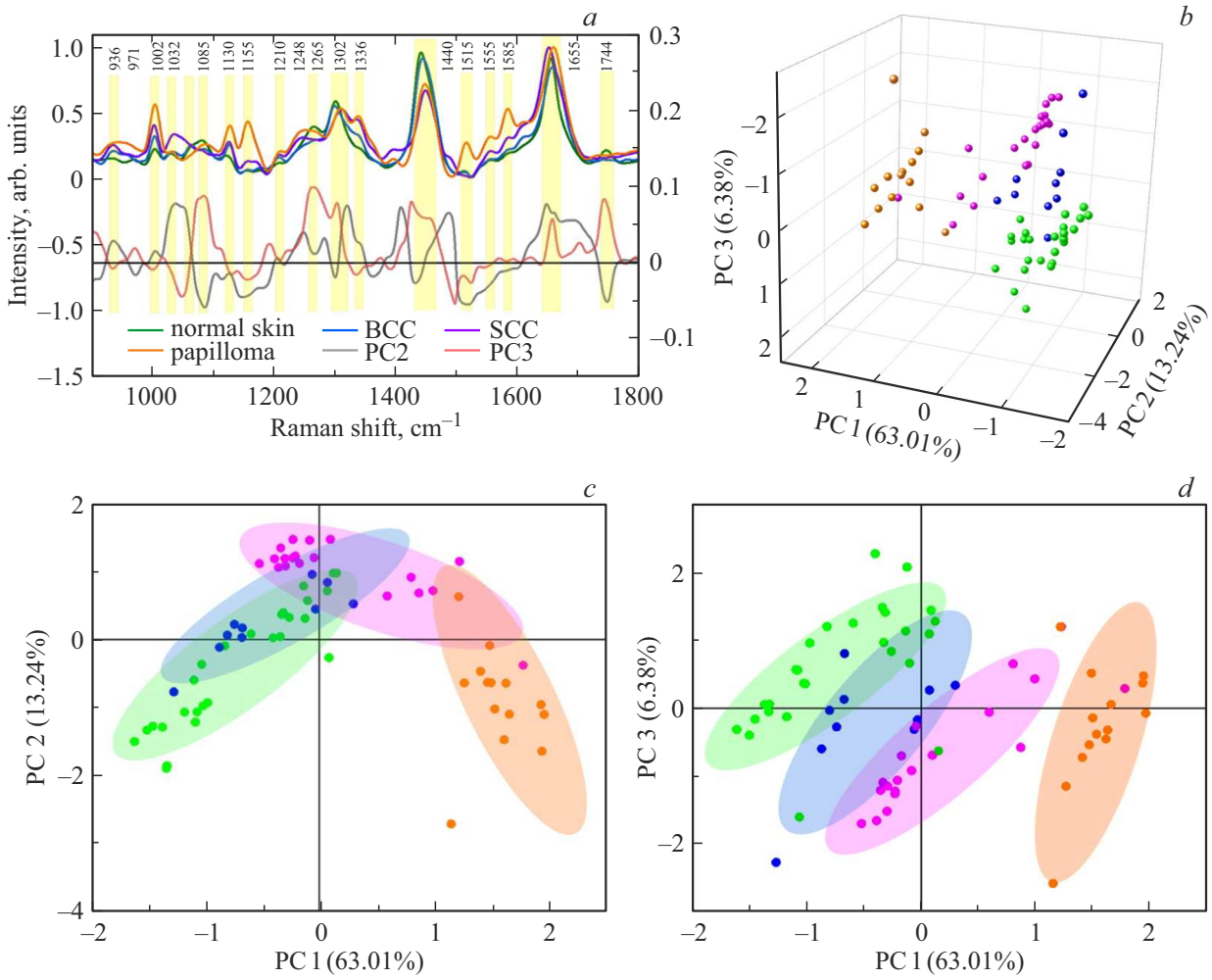

Figure 1. (*a*) RS spectra of natural skin (green line), BCC (blue line), SCC (pink line) and papilloma (orange line) in 532 nm laser excitation (left-hand vertical scale) and highlighted main components (loads) (PC2, gray line; PC3, red line; right-hand vertical line). Distribution of coefficients (counts) for the three first components in the form of a 3D diagram (*b*) and its projections (*c, d*); marker colors correspond to line colors in the figure (*a*).

skin, 7 BSS, 5 SCC, 3 papilloma samples). For each sample, 10 to 15 spectra were measured.

The RS spectra were measured using Renishaw inVia Basis spectrometer (inVia InSpect, Renishaw) with 532 nm and 785 nm wavelengths. When measuring 532 nm excitation spectra, power up to 20 mW was used, acquisition time was 2 s. Measurements at 785 nm were carried out at 45 mW and acquisition time 10 s [8]. For 532 nm excitation wavelength, a lower laser power and shorter exposure shall be used to avoid the failure of biological samples. These operating conditions were chosen as the best possible ones that do not result in visible damage of the samples and ensure good signal-to-noise ratio. Morphology of skin tissue samples remained without visible changes and has no signs of laser scarring after laser exposure.

Spectra processing included removal of the fluorescence background and spectra smoothing in OriginPro software suite (OriginPro 2019b 9.6.5.169). The sample spectra were divided into groups by the histopathology results, then the principal component analysis was used. PCA is the method that converts potentially correlated variables to a lower number of non-correlated variables — principal components. Diagrams of the obtained principal components (loads) vs. wave numbers help describe biochemical differences in RS spectra and illustrate various groups of spectra corresponding to normal skin and tumors. We have addressed the main known bands in RS spectra typical for various biotissue molecule vibrations and compared this information with values from the principal component curves in the corresponding spectral bands.

Results and discussion

This section provides the PCA results for RS spectra of normal skin and skin tumor samples measured with excitation at 532 nm and 785 nm, and the differentiation results based on the first three principal components.

Table 1. The main molecular vibration bands in the RS spectra at 532 nm excitation wavelength and corresponding values on the principal component diagrams

RS band, cm^{-1}	Explanation	Content	PC2	PC3	Source
936	ν(CC)	Proteins (α-*helix*), collagen	+	−	[12]
971	ν(C−C)	phospholipids	−	+	[13]
1002	ν(CProteins −C), phenylalanine	(*Phe*), carotenoids	+	−	[8,11–13]
1032	δ(CHProteins $_2CH_3$), phenylalanine, proline		+		[13]
1085	ν(CC), ν(CN)	Lipids, proteins, nucleic acids	−	+	[11]
1130	ν(CC), ν(CN)	Lipids, proteins, ceramides		−	[8,11,14]
1155	ν(CC), Proteins ν(CN)	, carotenoids	−	−	[11,14]
1210	ν(C-C_6H_5), phenylalanine, thymine, adenine, amide III	Proteins(*Phe*)			[11,15]
1248	amide III	Proteins (α-*helix*), collagen, elastin	+		[16]
1265	amide III (α-*helix*), ν(CN)	Proteins(α-*helix*), collagen, elastin, keratin		+	[14,16]
1301	τ(CH_2, CH_3)	Lipids, proteins, triolein	→	←	[11,14,16,17]
1336	ω(CH_2, CH_3)	Lipids, proteins, elastin nucleic acids		−	[11,14]
1440	δ(CH_2), δ(CH_3)	Lipids, proteins, triolein	→	←	[11,14,16]
1515	ν(C=C)	Carotenoids	−		[11,18]
1555	ν(C=C)	tryptophan			[8,14,15]
1585	δ(C=C), ν(C=C)	phenylalanine, Proteins(*Phe*)			[8,14,19,20]
1655	amideI, ν(C=C)	Lipids, proteins (α-*helix*), triolein	←	+	[8,11,14,16,21]
1744	ν(C=O)	Lipids		→	[8,11,22]

1. PCA analysis at 532 nm laser excitation

The spectral lines were interpreted using the literature data [8–17], see Table 1 for details. These lines, measured middle RS spectra for each type of samples at 532 nm excitation wavelength and principal component (load) curves #2 (PC2) and #3 (PC3) are shown in Figure 1, *a*. Principal component #1 contains spectral bands typical for all samples and does not show significant difference between groups [18].

Thus, the positive component of PC2 mainly includes the bands (marked with „+“ in column PC2 Table 1) assigned to proteins and correlates with spectral features of BCC and SCC (mean coefficients (counts) are equal to 0.13 and 1.05, respectively); the negative component contains the bands (marked with „−“ in Table 1) assigned to proteins and lipids and correlates with RS spectra of normal skin and papilloma (mean coefficients (counts) are equal to −0.38 and −0.89, respectively). The positive component of PC3 (bands marked with „+“ in column PC3 Table 1) correlates with proteins and lipids and mainly represents a normal skin count dispersion area (mean coefficient is 0.78); the negative component correlates with proteins and carotenoids and is associated with skin malignancies (mean coefficients are −0.33, −0.65 and −0.26 for BCC, SCC and papilloma, respectively). In addition, PC2 and PC3 components are responsible for peak shifts in bands 1302, 1440 and 1650 cm^{-1} (marked with „→“ and „←“ in Table 1).

To confirm the relevance and sufficiency of highlighted spectral features for differentiation between normal skin and tumors, classification efficiency using *MATLAB Classification Learner* (R2022b, *MathWorks*) was assessed. Linear discriminant analysis and quadratic discriminant analysis (LDA and QDA, respectively) [8,23] were used for the three first principal components (PC) and their efficiency was assessed using classification matrices and ROC (*receiver operating characteristic* curves) [8,24–27]. Results for four skin tissue classes (normal skin, BCC, SCC and papilloma) are shown in Figure 2.

ROC curves (Figure 2, *a* and *b*) display the changes in the true-positive results level compared with false-positive results level with different separation thresholds for each

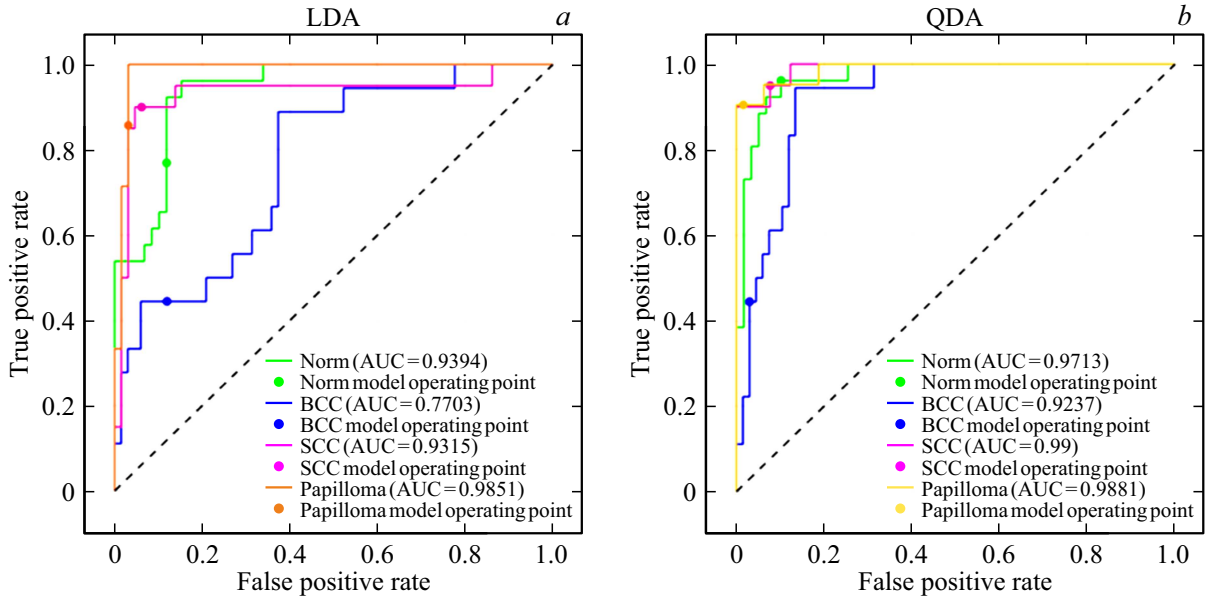

c

	Normal	BCC	SCC	Papilloma
Normal	76.9	23.1		
BCC	38.9	44.4	16.7	
SCC			90	10
Papilloma		9.5	4.8	85.7

d

	Normal	BCC	SCC	Papilloma
Normal	96.2	3.8		
BCC	33.3	44.4	16.7	5.6
SCC		5	95	
Papilloma			9.5	90.5

Figure 2. Classification of normal skin, BCC, SCC and papilloma samples *in vitro* at 532 nm laser excitation using linear (*a*, *c*) and quadratic (*b*, *d*) discriminant analysis. ROC — curves with AUC values for normal skin, BCC, SCC and papilloma (*a*, *b*); *c*, *d* — corresponding classification matrices (percentage values are given).

sample class. ROC AUC (*area under curve*) estimates indicate the general method efficiency, in particular, normal skin, BCC, SCC and papilloma values were equal to 0.94, 0.77, 0.93 and 0.99, respectively, when using LDA, and a little higher — 0.97, 0.92, 0.99 and 0.99, respectively, for QDA. Classification matrices (Figure 2, *c* and *d*) show the probability of assignment to any class as a result of classification (predicted class) depending on the true class for optimum separation thresholds; diagonal values correspond to true classification data for each class. Thus, SCC was correctly detected in 90% (LDA) and 95% (QDA) cases, while normal skin was correctly classified in 76.9% (LDA) and 96.2% (QDA) cases. Partial overlapping of dots cluster classified as BCC with clusters representing normal skin and SCC (Figure 1) hinders their efficient separation using the discriminant analysis that results in quite low degree of correct classification (44.4%) for BCC.

2. PCA with 785 nm laser excitation Comparison data of molecular vibration bands with principal component values are listed in Table 2. Middle RS spectra for each type of samples at 785 nm excitation wavelength and principal component (load) curves #2 (PC2) and #3 (PC3) are shown in Figure 3, *a*.

As shown in Table 2 (marked with „+“ and „−“), the positive component of PC2 includes protein and lipid bands typical for normal skin and BCC (mean coefficients (counts) are equal to 0.92 and 0.62,respectively); the negative component includes protein and carotenoid components whose bands coincide with the spectral features of SCC (mean coefficient is −0.28) and papilloma (−1.32). The positive component of PC3 may be assigned to proteins, it reflects to a great extent the SCC features (mean coefficient is 1.6) and BCC features (0.21); the negative component includes lipids, proteins and carotenoids and correlates with the spectral features of natural skin and papilloma (mean coefficients are − 0.48 and − 0.77, respectively).

Similar to the data obtained at 532 nm, RS spectra of various classes of samples demonstrate significant differences at 785 nm, and, thus, representative features have been identified using PCA, and normal skin and tumors were efficiently classified using LDA and QDA for the three first PC (Figure 4). ROC curves shown in Figure 4, *a* and *b* indicate that classification using spectra at 785 nm

Table 2. The main molecular vibration bands in the RS spectra at 785 nm excitation wavelength and corresponding values on the principal component diagrams

RS band, cm^{-1}	Explanation	Content	PC2	PC3	Source
proteins 936	ν(CC)	(α-*helix*), collagen	+	+	[12]
971	ν(C−C)	phospholipids	+	−	[13]
1002	ν(CProteins −C), phenylalanine	(*Phe*), carotenoids		−	[8,11-13]
proteins1032	$\delta(CH_2CH_3)$, phenylalanine, proline		←	+	[13]
1062	ν(CC)	Lipids, ceramides	+		[14,16]
1082	ν(CC), ν(CN)	phospholipids, nucleic acids, triolein		−	[11]
1130	ν(CC), ν(CN)	Lipids, proteins, ceramides			[8,11,14]
1155	ν(CC), ν(CN)	Proteins, arotinoids	−	−	[11,14]
1210	$\nu(C\text{-}C_6H_5)$, phenylalanine, thymine, adenine, amide III	Proteins(*Phe*)		+	[11,15]
1248	amide III	Proteins (α-*helix*), collagen, elastin			[16]
1265	amide III (α-*helix*), ν(CN)	Proteins (α-*helix*), collagen, elastin, keratin		−	[14,16]
1301	$\tau(CH_2, CH_3)$		+	−Lipids, proteins, triolein	[11,14,16,17]
1336	$\omega(CH_2, CH_3)$	Lipids, proteins, nucleic acids, elastin			[11,14]
1440	$\delta(CH_2)$, $\delta(CH_3)$	Lipids, proteins, triolein	←	→	[11,14,16]
1517	ν(C=C)	Carotenoids	−	−	[11,18]
1555	ν(C=C)	tryptophan			[8,14,15]
1582	δ(C=C), phenylalanine, Proteins(*Phe*) ν(C=C)			[8,14,19,20]	
1655	amideI, ν(C=C)	Lipids, proteins(α-*helix*), triolein	←	←	[8,11,14,16,21]
1744	ν(C=O)	Lipids	+	−	[8,11,22]

excitation wavelength is more reliable than that based on data obtained at 532 nm. Actually, ROC AUC LDA data for normal skin, BCC, SCC and papilloma classes were equal to 0.98, 0.99, 0.996 and 1, respectively; for QDA, they were 0.996, 0.99, $\sim$ 1 and 1. According to the classification matrices (Figure 4, *c* and *d*), SCC and papilloma may be properly distinguished rom normal skin and BCC in all cases for the both types of analysis. True classification data for normal skin and BCC were 76 and 82.4%, respectively, for LDA and achieved 92% and 88.2% for QDA. Despite overlapping of regions corresponding to different classes in PC projections (Figure 3, *c* and *d*), they may be separated in 3D space (Figure 3, *b*) resulting in better classification of BCC and normal skin tissue than at 532 nm.

Conclusion

The study performed *in vitro* analysis of RS spectra of skin malignancies using the principal component method and interpretation of highlighted spectral features in accordance with the known data on molecular vibrations. According to the findings, the positive component of PC2 at 532 nm mainly includes proteins and correlates with SCC features, while the negative component includes proteins and lipids correlating with the spectral features of normal skin and papilloma. The positive component of PC3 includes proteins and lipids whose spectral features correspond to normal skin; the negative component contains protein and carotenoid features associated with tumors. At 785 nm, the positive component of PC2 corresponds to proteins and lipids and includes spectral features of normal skin and BCC; the negative component corresponds to proteins and carotenoids, including SCC and papilloma features. The positive component of PC3 includes proteins corresponding to SCC and BCC features, while the negative component indicates lipids, proteins and carotenoids corresponding to normal skin and papilloma. Analysis of individual spectral bands shows that the identified features are similar at 532 nm and 785 nm laser excitation, however, signal-to-noise ratio for 785 nm is higher due to lower background fluorescence. excitation at 785 nm results in considerable increase in RS intensity of particular vibration modes corresponding to chromophores that absorb near this excitation wavelength. As a result, the differences between

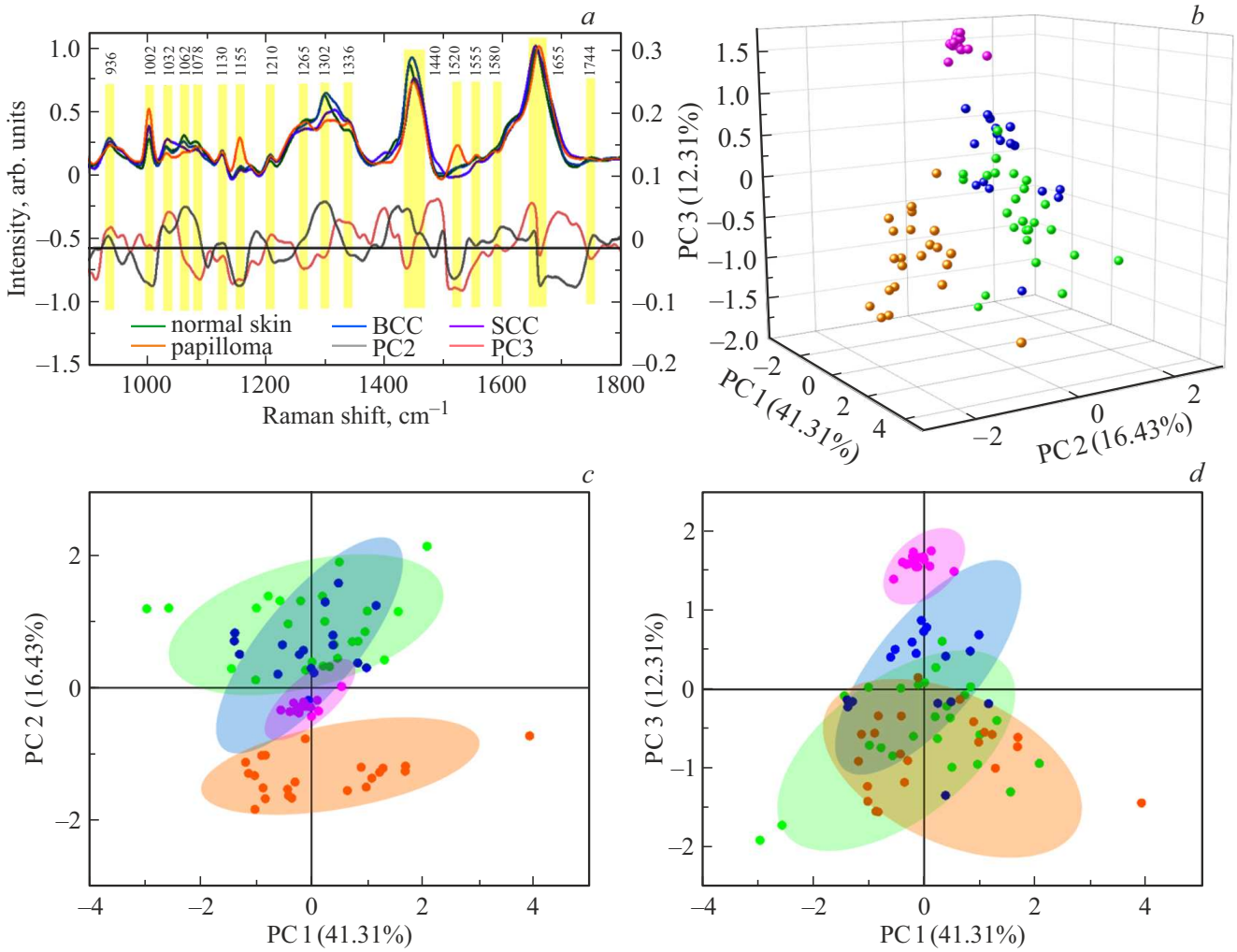

Figure 3. (*a*) RS spectra of natural skin (green line), BCC (blue line), SCC (pink line) and papilloma (orange line) in 785 nm laser excitation (left-hand vertical scale) and highlighted main components (loads) (PC2, gray line; PC3, red line; right-hand vertical line). Distribution of coefficients (counts) for the three first components in the form of a 3D diagram (*b*) and its projections (*c, d*); marker colors correspond to line colors in the figure (*a*).

the RS spectra of normal skin and tumors (BCC, SCC) may be associated with the change in protein structure in tumor cells as well as with the decrease in the intensity of lipid-specific bands. Therefore, the differential diagnosis using RS spectra measures at 785 nm is more reliable than at 532 nm and achieves the probability of correct classification higher than 92%. The addressed methods may be used in the same way for *in vivo* analysis and differentiation and, if the corresponding RS spectra measurement equipment is present, may be the basis for creation of automated systems for noninvasive express diagnosis of skin neoplasms. Further development of tools for early detection by the RS spectroscopy methods may be associated with multispectral data processing (at different excitation wavelengths) and extension of the test vibration peak range.

Compliance with ethical standards

The study was carried out in accordance with the Declaration of Helsinki and approved by the Inter-University Ethics Committee of A.I. Yevdokimov Moscow State University of Medicine and Dentistry, Ministry of Health of the Russian Federation (Moscow, Russia, report code 3, 16.03.2023) for human research. Informed consent was received from all research participants.

Funding

The authors are grateful to the Russian Science Foundation for the financial support of the research under project № 23–25–00249.

Conflict of interest

The authors declare that they have no conflict of interest.

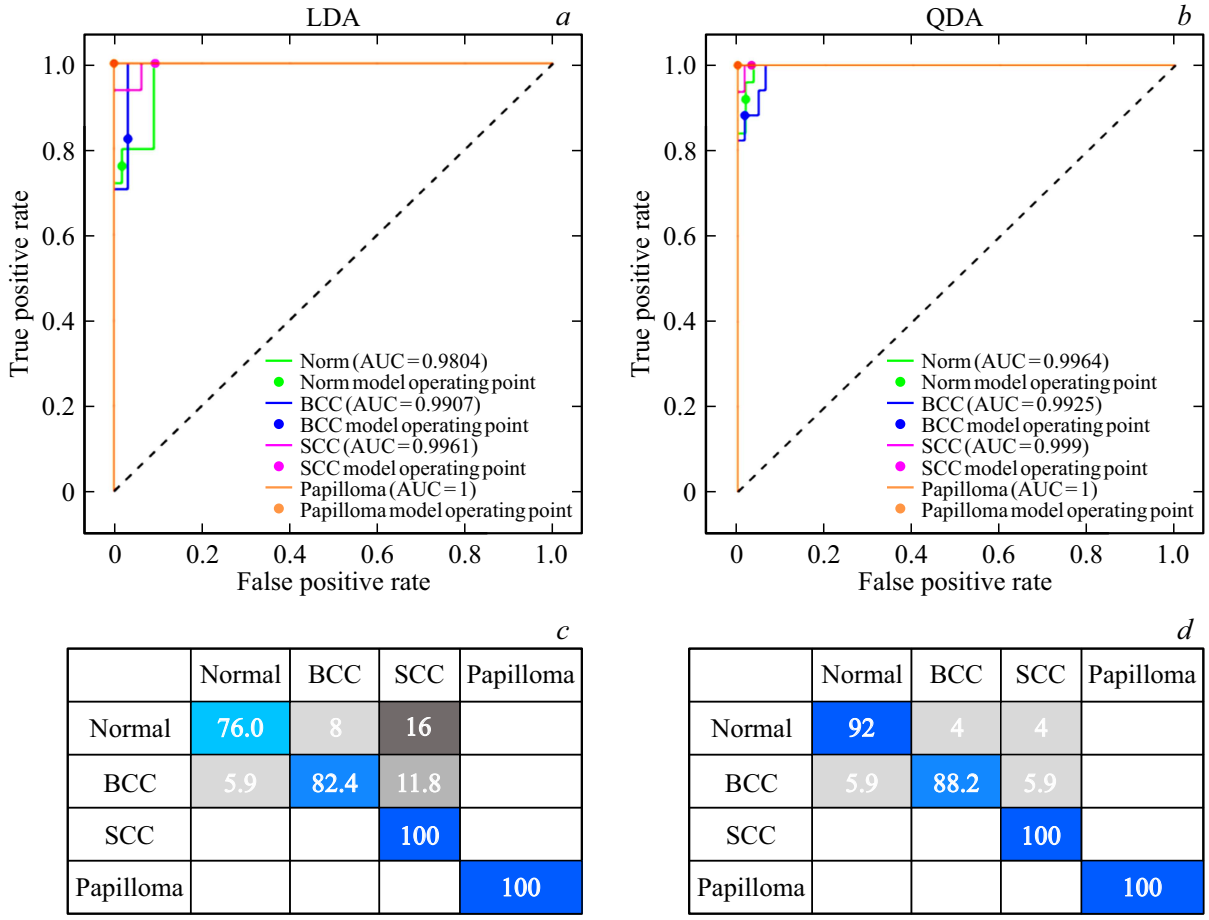

	Normal	BCC	SCC	Papilloma
Normal	76.0	8	16	
BCC	5.9	82.4	11.8	
SCC			100	
Papilloma				100

	Normal	BCC	SCC	Papilloma
Normal	92	4	4	
BCC	5.9	88.2	5.9	
SCC			100	
Papilloma				100

Figure 4. Classification of normal skin, BCC, SCC and papilloma samples *in vitro* at 785 nm laser excitation using linear (*a, c*) and quadratic (*b, d*) discriminant analysis. ROC — curves with AUC values for normal skin, BCC, SCC and papilloma (*a, c*); corresponding classification matrices (percentage values are given) (*c, d*).

References

[1] R.L. Siegel, K.D. Miller, A. Jemal. CA: a cancer journal for clinicians, **73**, 17 (2023). DOI: 10.3322/caac.21763

[2] E.N. Rimskaya, A.O. Shchad'ko, I.A. Apollonova, A.P. Nikolaev, A.N. Briko, I.A. Deshin, P.Yu. brezhnoy, K.G. Kudrin, K.I. Zaitsev, V.V. Tuchin, I.V. Reshetov. Opt. i spektr., **126** (5), 584 (2019). (in Russian) DOI: 10.21883/OS.2019.05.47657.6-19

[3] A. Eggermont, A. Spatz, C. Robert. The Lancet, **1** (383), 816 (2014). DOI: 10.1016/S0140-6736(13)60802-8

[4] J. Muller, J. Hartmann, C. Bert. Phys. in Medicine & Biology, **61** (7), 2646 (2016). DOI: 10.1088/0031-9155/61/7/2646

[5] V. Neuschmelting, N.C. Burton, H. Lockau, A. Urich, S. Harmsen, V. Ntziachristos, M.F. Kircher. Photoacoustics, **4** (1), 1 (2016). DOI: 10.1016/j.pacs.2015.12.001

[6] N. MacKinnon, F. Vasefi, N. Booth, D.L. Farkas. Proc. of SPIE, **9711** (1), 971111 (2016). DOI: 10.1117/12.2222415

[7] K.I. Zaytsev, K.G. Kudrin, V.E. Karasik, I.V. Reshetov, S.O. Yurchenko. Appl. Phys. Lett., **106** (5), 053702 (2015). DOI: 10.1063/1.4907350

[8] E. Rimskaya, S. Shelygina, A. Timurzieva, I. Saraeva, E. Perevedentseva, N. Melnik, K. Kudrin, D. Reshetov, S. Kudryashov. International J. Mol. Sci., **24**, 14748 (2023). DOI: 10.3390/ijms241914748

[9] G.F. Silveira, D.M. Strottmann, L. de Borba, D.S. Mansur, N.I.T. Zanchin, J. Bordignon, C.N. Duarte dos Santos. Clinical and Experimental Immunology, **183** (1), 114 (2016). DOI: 10.1111/cei.12701

[10] E.G. Borisova, I.A. Bratchenko, Y.A. Khristoforova, L.A. Bratchenko, T.I. Genova, A.I. Gisbrecht, A.A. Moryatov, S.V. Kozlov, P.P. Troyanova, V.P. Zakharov. Optical Engineering, **59**, 061616 (2020). DOI: 10.1117/1.OE.59.6.061616

[11] A. Synytsya, M. Judexova, D. Hoskovec, M. Miskovicova, L. Petruzelka. J. Raman Spectrosc., **45**, 903 (2014). DOI: 10.1002/jrs.4581

[12] M.S. Bergholt, W. Zheng, K. Lin, Z. Huang, K.Y. Ho, K.G. Yeoh, Mi. Teh, J.B.Y. So. J. Biomedical Optics, **16** (3), 037003 (2011). DOI: 10.1117/1.3556723

[13] L. Shang, J. Tang, J. Wu, H. Shang, X. Huang, Y. Bao, Z. Xu, H. Wang, J. Yin. Biosensors, **13**, 65 (2023). DOI: 10.3390/bios13010065

[14] S. Tfaili, C. Gobinet, G. Josse, J.F. Angiboust, M. Manfait, O. Piot. Analyst, **137**, 3673 (2012). DOI: 10.1039/C2AN16292J

[15] Z.W. Huang, A. Mcwilliams, H. Lui, D.I. McLean, S. Lam, H. Zeng. International J. Cancer, **107** (6), 1047 (2003). DOI: 10.1002/ijc.11500.

[16] X. Feng, A.J. Moy, H.T. Nguyen, J. Zhang, M.C. Fox, K.R. Sebastian, J.S. Reichenberg, M.K. Markey, J.W. Tunnell. Biomedical Optics Express, **8**, 2835 (2017). DOI: 10.1364/BOE.8.002835
[17] R. Vyumvuhore, A. Tfayli, H. Duplan, A. Delalleau, M. Manfait, A. Baillet-Guffroy. Analyst, **138**, 4103 (2013). DOI: 10.1039/c3an00716b
[18] L. Silveira, S. Sathaiah, R.A. Zangaro, M.T. Pacheco, M.C. Chavantes, C.A. Pasqualucci. Lasers in Surgery and Medicine, **30** (4), 290 (2002). DOI: 10.1002/lsm.10053
[19] P.J. Caspers, H.A. Bruining, G.J. Puppels, G.W. Lucassen, E.A. Carter. J. Investigative Dermatology, **116**, 434 (2001). DOI: 10.1046/j.1523-1747.2001.01258.x
[20] J. Anastassopoulou, M. Kyriakidou, E. Malesiou, M. Rallis, T. Theophanides. In Vivo, **33**, 567 (2019). DOI: 10.21873/invivo.1151.
[21] M. Gniadecka, H.C. Wulf, N. Nymark Mortensen, O. Faurskov Nielsen, D.H. Christensen. J. Raman Spectrosc., **28**, 125 (1997). DOI: 10.1002/(SICI)1097-4555(199702)28:2/3 ¡125::AID-JRS65¿3.0.CO;2-%23
[22] P. Rekha, P. Aruna, E. Brindha, D. Koteeswaran, M. Baludavid, S. Ganesan. J. Raman Spectrosc., **47**, 763 (2016). DOI: 10.1002/jrs.4897
[23] C. Yorucu, K. Lau, S. Mittar, N.H. Green, A. Raza, I.U. Rehman, S. MacNeil. Appl. Spectrosc. Rev., **51** (4), 243 (2016). DOI: 10.1080/05704928.2015.1126840
[24] S. Sigurdsson, P.A. Philipsen, L.K. Hansen, J. Larsen, M. Gniadecka, H.C. Wulf. IEEE Transactions on Biomedical Engineering, **51**, 1784 (2004). DOI: 10.1109/TBME.2004.831538
[25] X.Y. Liu, P. Zhang, L. Su, L.M. Wang, X.D. Wei, H.Q. Wang, T.F. Ling. J. Nanoscience and Nanotechnology, **18**, 6776 (2018). DOI: 10.1166/jnn.2018.15510
[26] I.A. Bratchenko, L.A. Bratchenko, A.A. Moryatov, Y.A. Khristoforova, D.N. Artemyev, O.O. Myakinin, A.E. Orlov, S.V. Kozlov, V.P. Zakharov. Experimental Dermatology, **30**, 652 (2021). DOI: 10.1111/exd.14301
[27] C.A. Lieber, S.K. Majumder, D. Billheimer, D.L. Ellis, A.J. Mahadevan-Jansen. Biomedical Opt., **13**, 024013 (2008). DOI: 10.1117/1.2899155

Translated by E.Ilinskaya